

Int. J. Electrochem. Sci., 14 (2019) 9825 – 9837, doi: 10.20964/2019.10.02

International Journal of
**ELECTROCHEMICAL
SCIENCE**

www.electrochemsci.org

Electric Conductivity of Electrolytic Copper Powder Filled Poly(Lactide-co-Glycolide) Composites

Miroslav M. Pavlović^{1,*}, Radoje V. Pantović², Zoran Janković³, Dragan Nedeljković⁴,
Nebojša D. Nikolić¹, Miomir G. Pavlović¹ Jasmina S. Stevanović^{1,5}

¹ Institute of Chemistry, Technology and Metallurgy, Department of Electrochemistry, University of Belgrade, Belgrade, Serbia

² Technical Faculty in Bor, University of Belgrade, Bor, Serbia

³ V&Z Zaštita, d.o.o., B. Luka, Republic of Srpska, Bosnia and Herzegovina

⁴ European university, Faculty of international engineering management, Belgrade, Serbia

⁵ Center of Excellence in Environmental Chemistry and Engineering - ICTM, University of Belgrade, Belgrade, Serbia

*E-mail: mpavlovic@tmf.bg.ac.rs

Received: 26 June 2019 / *Accepted:* 3 August 2019 / *Published:* 30 August 2019

This manuscript presents the results of investigating the properties of composite materials having poly(lactide-co-glycolide) (PLGA) matrix filled with electrolytically produced copper powder whose particles have a highly developed branched structure. The volume fraction of the copper powder used as a filler for the preparation of the composite was varied from 0.4 to 7.2 vol. %. The samples were prepared at 140 °C by hot molding injection. The effect of the morphology of electrolytically obtained copper powder on the appearance of the percolation threshold and on the conductivity of the composites was studied. Characterization included impedance spectroscopy (IS) measurement of electric conductivity and scanning electron microscopy (SEM), energy dispersive X-ray spectroscopy (EDS), and Fourier-transform Infrared Spectroscopy (FTIR) morphological analysis. Electric conductive pathways were formed throughout the entire volume of the composites, where their formation was purely stochastic in all the dimensions. The percolation threshold was 2.72 vol.%, which is significantly lower than the one stated in the literature for similar composites, since these kind of composites are investigated for the first time. This property can be attributed to the use of a filler of different, diverse morphologies.

Keywords: electrical conductivity; biodegradable composite material; Poly(lactide-co-glycolide); electrolytic copper powder; FTIR; hardness.

1. INTRODUCTION

Electronic devices have crucial roles in everyday lives in modern society. Although these electronic devices offer vigorous and consistent operation with durable service and shelflife, the ever fast enhancement that comes by hand with the prompt proliferation leads to increasing amounts of electronic waste, also known as e-waste. This e-waste grows each year by more than 50 Mt [1,2]. In recent years, global focus was striving towards disposal, recycling and reusing of e-waste [3,4]. Potential solution to this problem comes in the form of “transient electronics” [5–9]. Transient electronic devices, unlike conventional devices that are built to last, physically disintegrate after relatively short and, what is more important, controlled lifetime when they are subjected to specific environment elements. These elements include, but are not limited to: water and other biofluids [5,9–11], moisture [12], light [13] and heat [14–17]. This transiency is manifested by diminishing of physical and electronic properties, and it is mostly programmable by material selections [12,18].

New type of electronics, being environmentally and ecologically friendly and having the ability to be dissolved and disintegrated either by microorganisms or in water and different biofluids are called bioresorbable electronics. These dissolution and disintegration products are completely nonthreatening, and different types of bioresorbable materials are used for manufacturing bioresorbable electronic devices. These materials are usually biodegradable polymers, conductors, semiconductors and dielectrics [5,19]. Up until now, production and processing of these materials was performed by vacuum-based fabrication methods.

Bioresorbable electronic devices have mainly found applications in biomedicine. They are used for health monitoring [20], sensing [21,22] and drug delivery [23,24], but the range for using these new devices is growing by day.

Poly(lactide-co-glycolide) or PLGA is biodegradable copolymer usually synthesized by ring-opening co-polymerization of glycolic acid (GA) and lactic acid (LA). Depending on the ratio of LA to GA used in the process of polymerization, different forms of PLGA that are identified by the molar ratio of the starting LA and GA monomers can be obtained [5]. PLGA is the most often used synthetic biocompatible and biodegradable polymer. American Food and Drug Administration (FDA) has approved vast number of medical devices that consist of or that are partially made of PLGA. [25]. PLGA degradation rate can be controlled much easier compared to the homopolymers of poly(lactic acid) and poly(glycolic acid) [26,27]. This great level of degradation control has made PLGA one of the favorite candidates for use as a material for bone regeneration. Hence its application goes from fibers, scaffolds, micro- and nanospheres and coatings in different medical requirements. PLGA can be completely amorphous, completely crystalline and all the variations in between, which depends on block structure and molar ratio of LA and GA monomers [28]. Glass transition temperature of different PLGAs are in the range of 40-60 °C. In living systems PLGA slowly degrade into natural metabolites, such as lactic and glycolic acids. Besides the drawback of PLGA having low surface energy and high hydrophobicity, and hence being poor substrate for cellular attachment and growth [29,30], it is most widely used among the various available biodegradable polymers for different medical applications that include drug delivery, bone screws and other tissue replacement implants. The last decades have cast light and brought great progress in the field of electroconductive polymers filled with different

metal and other conductive filler powders. The addition of a conductive base as filler in a polymer matrix allows the retention of polymer mechanical properties while the composite prepared in this manner is gaining the electrical properties of the metal [31]. Conductivities of these polymer composites are largely dependent on few factors. Firstly, it is affected by the nature and morphology of the contact between the filler particles, and, secondly it is essentially dependent on the volume fraction of the conductive particles. This is well explained by the percolation theory [32–37].

Despite the progress and improvements in percolation theory, systems with conductive fillers with highly branched surfaces have not been examined in much details. Also, electrical conductivity and electrical behavior of composite systems with biodegradable polymers matrices have not been studied a lot in the literature. According to authors' knowledge PLGA systems filled with conductive powders have not been studied before, and this finding has led to investigation and detailed study of real synergetic effects of fillers dimensionalities suitable for construction of conductive networks in conductive biodegradable PLGA composites. The selection was carried to galvanostatically produced copper powder with highly dendritic and branched surface.

Motivation for development of highly conductive PLGA composites laid in the desire to obtain copper filled polymer-based materials that would retain biodegradability, ease of processing, and that would provide high values of electric conductivity at low cost. Hence, in order to achieve these characteristics, highly branched and dendritic copper filler was produced and used for preparation of PLGA/Cu composites in order to reach low percolation threshold and the results of electrical conductivity of these composites are shown in this paper.

2. EXPERIMENTAL

In the experimental part of the work, ester terminated Poly(D,L-lactide-co-glycolide) (PLGA) with lactide to glycolide ratio of 85:15 was used as matrix for prepared composites. PLGA polymer was used as commercially available powder supplied by Sigma-Aldrich. PLGA had average molecular weight of $M_w \sim 190,000\text{--}240,000 \text{ g mol}^{-1}$, with a density of 1.27 g cm^{-3} , and the electrical conductivity of $9.8 \times 10^{-11} \text{ S cm}^{-1}$.

In the production of copper powders, acid electrolytes with lower copper concentrations and higher working current densities are preferred, as compared to the corresponding electrolytes for copper refinement. The conditions for copper powder production in galvanostatic electrolysis regime is shown in Table 1. Electrodes material was copper, and electrolytes were prepared from p.a. chemicals (Merck) and demineralized water. Brushing of cathodes was performed in order to remove powder after precipitation process. The powder was then washed, protected from oxidation, and the stabilization and drying processes were performed.

Table 1. Electrolysis regime conditions for galvanostatic copper powder production

j (A m^{-2})	τ_r (min)	Q (vol/h)	t ($^{\circ}\text{C}$)	$c(\text{Cu}^{+2})$ (g dm^{-3})	$c(\text{H}_2\text{SO}_4)$ (g dm^{-3})
3600	20	1.5	50 ± 2	13	145

Large quantities of double-distilled water were used for copper powder washing. Washing was performed at 25 °C until the powder was acid free, and then it was washed with 1 g dm⁻³ aqueous solution of a benzoic acid (Sigma-Aldrich). Benzoic acid was used as corrosion inhibitor, preventing the powder from succeeding oxidation. Further, the Cu powder was dried in dynamic N₂ filled tunnel furnace at 130 °C. Finally, the produced copper powder was sieved through mesh with openings of 45 μm.

Apparent density measurements and quantitative microstructural analyses were performed on the obtained powders under these conditions. Apparent density was determined according to ISO 3923-1979 (ratio between powder mass and volume of cylindrical vessel of 25 cm³). Then, the powder was sieved and for the same fraction the apparent density was determined one more time, as well as quantitative microstructural analysis and analysis of the morphology and structure of the particles by scanning electron microscopy (SEM). The quantitative microstructural analysis measurements were performed in order to conclude how the structure of the particle influences the bulk mass of the copper powder.

0.4 vol. % – 7.2 vol. % of copper powder filled PLGA polymer composites were prepared. Also, the reference samples consisting of pure PLGA and pressed copper powder were prepared. Poly(D,L-lactide-co-glycolide) was preheated and consecutively melted at $t = 140$ °C for the duration of 30 min, in order to reach steady state. Different amounts of copper powder were measured on analytical scale, and these amounts were added to heated, melted and stabilized PLGA melt. These mixtures were blended until the mixtures were fully homogenized. Homogenization was followed by samples production in the molder, model Atlas Polymer Evaluation Products LMM Model H30, and the samples were 4.8×10.3×13.3 mm. The prepared composites were left to cool down in the mold for 30 min at 25 °C. After removal from the mold, samples were polished with sandpaper and alumina slurry with Al₂O₃ particle sizes of 1 μm, 0.3 μm and 0.05 μm for conductivity measurements.

Electrical conductivity was measured by impedance spectroscopy (IS). Bio-Logic® SAS Instrument, model SP-200 operating in potentiostatic mode was used to measure electric conductivity on all prepared composites. Bio-Logic® was guided by EC-Lab® software. Measurements were performed in the manner that samples were put between two conductive metal plates made from copper and the response to sinusoidal signal of ±10mV (rms) was recorded. It needs to be mentioned that primary current density distribution was uniform and there was minimal or no effect of the edges due to geometry of the instrument contacts. ZView® software was used for treating and fitting experimental IS data. Scanning Electron Microscopy (SEM) analysis of PLGA composites and constituents was performed on Tescan Mira 3 XMU FEG-SEM. Jeol JSM 5800 SEM with a SiLi X-Ray detector (Oxford Link Isis series 300, UK) was used for obtaining EDS (energy-dispersive X-ray spectroscopy) data of the reference and composite samples. Michelson MB Series Bomen (Hartmann Braun) Fourier transform infrared spectroscopy (FTIR) was used for recording spectra in the range from 500 to 4000 cm⁻¹ of PLGA/Cu composites and the constituents. Nanoscope III Atomic Forces Microscope Multi Mode Scanning Probe Microscope (Digital Instruments) was used for logging topographies and morphologies of PLGA composites. Shore D hardness testing method was used for determining hardness of the PLGA composites at 25 °C. The method was used in accordance with ASTM D 2240-68 standard.

3. RESULTS AND DISCUSSION

Apparent density of electrodeposited copper powder, determined according to ISO 3923-1979, was 0.557 g cm^{-3} . Quantitative microstructural analysis of galvanostatically produced copper powder was performed in semi-automatic manner. The semi-automatic method was performed by principle of using digital board. The constituent profile is drawn using a cursor whose motion is registered by the microprocessor. The great advantage of these devices is that the human eye performs separation, and the experience of the operator allows the classification of constituents even in the case of very poor contrast. The results of quantitative microstructural analyses are shown in Table 2 and Figure 1, where the symbols that are used in the Table 2 have the meanings as follows:

- A (area) – Feature area of the particle
- D_{max} – Diameter of the largest particle.
- D_{min} – Diameter of the smallest particle.
- L_p - Perimeter
- f_A - Form area
- f_L - Form perimeter
- f_R - Roundness
- f_w – Ratio of the length of the polygon circumscribing the feature formed by tangents to its boundary

Table 2. Sieved fraction ($\leq 45\mu\text{m}$) characteristic parameters of galvanostatically deposited copper powder

	Max value	Min value	Mean value
A (area) (μm^2)	581.48	5.69	89.32
L_p (perimeter) (μm)	183.35	0.99	56.78
D_{max} (μm)	51.18	2.72	27.98
D_{min} (μm)	13.11	0.97	6.74
f_A (form area)	1.00	0.35	0.74
f_L (form perimeter)	0.87	0.11	0.51
f_w (waviness)	1.00	0.74	0.89
f_R (roundness)	4.01	1.21	2.11

From Figure 1 and from Table 2 it can be seen that produced copper powder used in the experiments has highly developed surface area. The data from Table 2 backup the later assertion, namely f_R which has the smallest values for circle, f_L and L_p values. f_R has values that are much higher than 1, which points to a conclusion that Cu powder has highly dendritic and branched structure. From Figure 1 it can be seen that Cu powder particles have well-developed primary and secondary dendrite arms. Quantitative microstructural analyses have shown that the angles between dendrite arms are typical for the face centered cubic crystals, which can be seen on Figure 1b. Also, as mentioned earlier, by analyzing f_L and L_p values it can be seen that copper powder particles are not very compact and rounded, but they have pronounced dendrite branching.

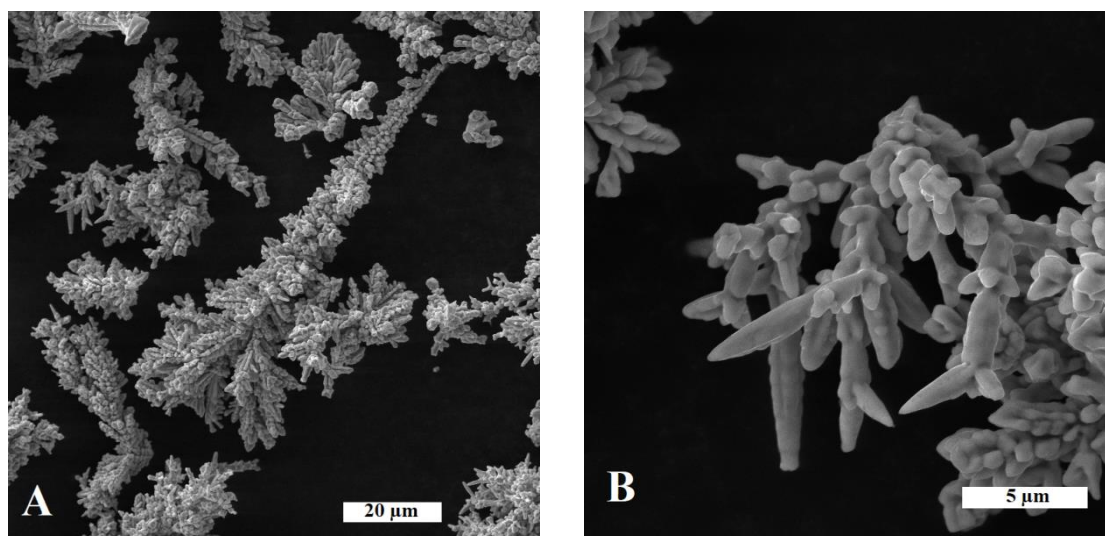


Figure 1. SEM images of a) galvanostatically produced and sieved Cu powder and b) single particle view of the same powder.

Morphology of produced and used copper powder is presented in Figure 1. Analyses of the images from Figure 1 show that Cu powder has very developed, branched and dendritic structure. Typical copper powder particle size is $< 45 \mu\text{m}$, which suits the fact that after production, the copper powder was sieved through mesh with openings of $45 \mu\text{m}$. The developed surface area of this copper powder makes this powder suitable candidate for the formation of a larger number of interparticle contacts between the conductive powder particles in the composite. It is assumed that it will lower the percolation threshold since presumably the particles have the ability to form multiple contacts with neighboring particles at lower filler volume fractions.

The electrical conductivity of the PLGA composites as a function of filler content was measured by impedance spectroscopy. Data treatment of the obtained results by ZView® software have shown presence of conductive pathways in the entire volume of the composite. Data treatment and fitting gives 8 branches with capacitors and resistors connected in parallel, representing these conductive pathways. By calculating equivalent capacitance and, most important, resistance using Equation 1, the electrical conductivity of the composites as a function of filler content for all the samples can be calculated.

$$\sigma = \frac{1}{\sum_1^7 R_i} \cdot \frac{l}{S} \quad (1)$$

In Equation 1 σ is electrical conductivity, R_i – resistivity of a layer in equivalent circuit, l – length and S – cross-section area of the sample. Plotting the data obtained and calculated from IS measurements for all composite samples in $\log \sigma$ vs. Φ plot, the conductivity curve of PLGA composites will be obtained, and this curve is shown in Figure 2.

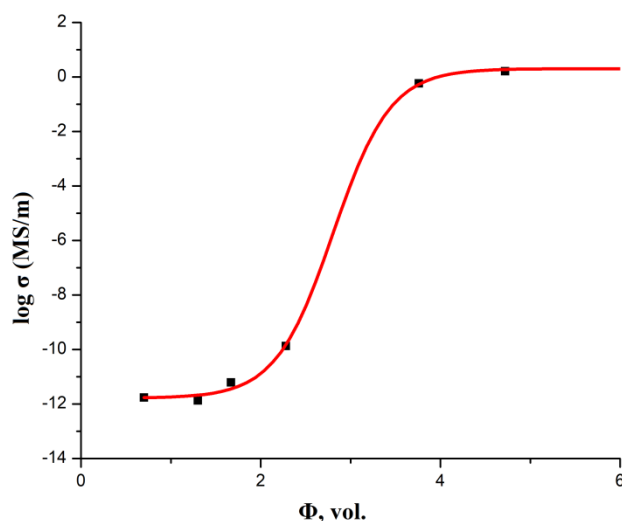


Figure 2. Change in electrical conductivity as a function of filler volume fraction for PLGA composites filled with copper powder

The conductivity of PLGA composites is showing typical S-shaped dependency of conductivity regarding volume fraction. This curve has three distinct regions, namely dielectric, transition and conductive. The way to obtain, and to calculate, the value of percolation threshold is to calculate the maximum value of the first derivative of the conductivity curve. The calculated value of percolation threshold, and the value that can be read from Figure 2, is 2.72 vol. %. This low percolation threshold value for PLGA composites is due to powder particles filler shape. Previous researches and investigations confirm the later statement [34,35,37,38]. As already shown in Figure 1 and Table 1 these particles are dendritic with well-developed surface area, and hence less filler was needed to form conductive network throughout the composite volume. If similar composite systems are compared, since PLGA/Cu composite system have never been studied before, especially not regarding electric conductivity, it can be seen from the literature overview that percolation threshold (PT) is much higher than 2.72 vol%, but the shape of highly conductive filler has smaller surface area, and the surface is not developed as in our case [39–43]. Nishi et al. [39] have obtained PT at 15 vol.% for PMMA/Cu systems, Osman et al. [40] have obtained 15 vol.% for PP/Al systems, Luyt et al. [41] have obtained 18.7 vol.% for both LDPE/Cu and LLDPE/Cu systems, while Baziard et al. [43] did not reach PT in their experiments, although the highest Cu content in epoxy/Cu system was 23,2 vol.%. Hence, it can be seen that more regular, rounded shapes of conductive filler lead to higher values of percolation threshold. Our previous experiments, together with results presented in this manuscript, lead to conclusion that the morphology of the particles plays a crucial role for the percolation threshold appearance. Besides the filler morphology, polymer matrix type, as well as preparation method influences the percolation threshold, which further moves towards lower values.

The cross section 4.8×13.3 mm in size of the sample at percolation threshold perpendicular to the surfaces at which the electrical conductivity was measured were made for further morphology examination of PLGA/Cu composites.. Figure 3 shows SEM image of the cross section of PLGA composite filled with copper powder at percolation threshold, where two different phases can be

observed. These phases are polymer phase (darker) and Cu branched conductive filler phase (lighter). In order to backup the statement of formation of conductive pathways throughout the polymer composite, and to determine mechanism of the electrical conductivity EDS measurements were performed on same cross section of PLGA/Cu composite. These measurements would give insight to interparticle contacts within composite mass. EDS results are shown in Figure 4.

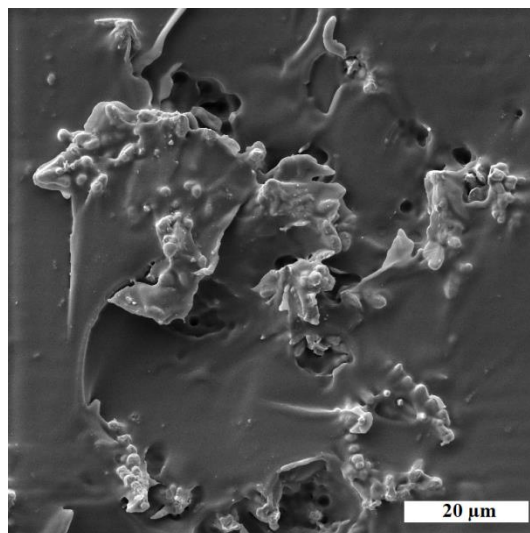


Figure 3. SEM image of cross section of PLGA/Cu composite at percolation threshold.

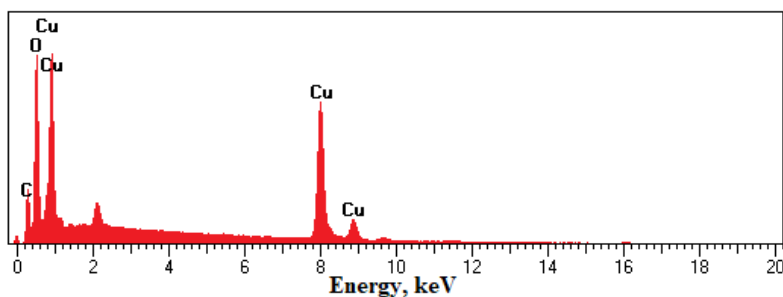


Figure 4. EDS spectrums of cross section of PLGA-Cu composite surface with polymer and filler phases analyses.

Besides point EDS analyses, the full surface analysis was also performed on the same cross section. Results of surface area EDS analysis are shown in Table 3.

Table 3. Elemental analysis of cross sections of PLGA/Cu composite at percolation threshold

Element type	Atomic %
C	48.12
O	43.11
Cu	8.77
Total	100

The morphology of polymer composite cross section characterized by the atomic force microscopy technique (AFM) in 2D and 3D view, as well as the morphology of a pure PLGA sample, are shown in Figure 5. As already mentioned and explained by SEM morphology analyse two different morphological surfaces characterized by different RMS roughness can be detected by careful analysis of the AFM images of tested polymer composites. The first morphology can be seen in labeled square in Figure 5b, and this surface morphology corresponds to copper powder. The RMS roughness of this part was 128 nm. The second morphology is shown in Figure 5c and corresponds to a polymer chain, i.e. pure PLGA polymer. The RMS roughness of this part is 51 nm. It is clear that higher RMS or Rq value of the first part was a consequence of a highly developed surface area of dendritic Cu powder particles. These claims were also proven by SEM technique.

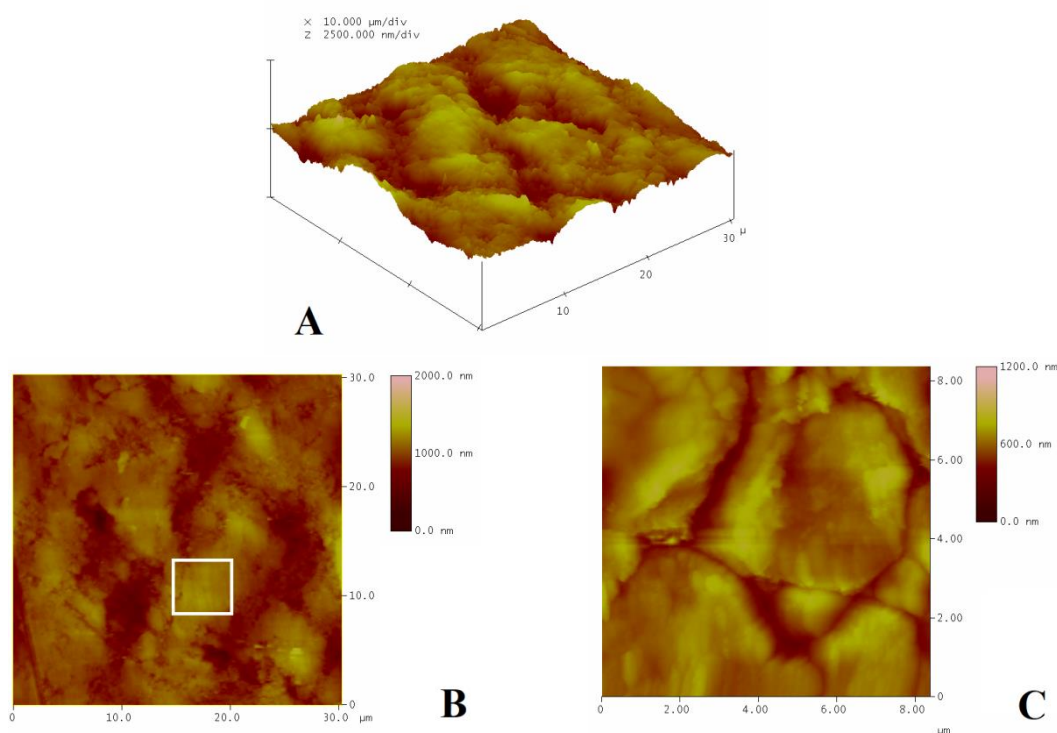


Figure 5. AFM images of PLGA composites filled with Cu powder at percolation threshold: a) 3D view of the composite, b) 2D image of the composite where the squared part of the image corresponds to Cu powder; c) AFM image of a pure PLGA polymer.

From the measurements of electric conductivity, and knowing that presented sample is conductive and at PT, the statement that conductive pathways are formed throughout the surface of the composite is proven. The size of copper phase present in the figures ($> 80 \mu\text{m}$) has larger value than the size of copper powder particles (which are $< 45 \mu\text{m}$ as seen from Figure 1) used for composite preparation. Clearly, composites conduct electricity through conductive pathways that are formed in 3D in pure stochastic order.

Figure 6 shows results of the results of FTIR measurements of the experiments performed on stabilized Cu filler, PLGA and its composite with 5.0 vol. % copper powder content. FTIR spectrum of

the Cu powder shows three distinct peaks at 3178.8 cm^{-1} and 1276 cm^{-1} characteristic for O-H groups from carboxylic part of benzoic acid, 1721.4 cm^{-1} characteristic for C=O groups from the carboxylic acid and around 1100 cm^{-1} characteristic for benzene ring. The FTIR results confirm that the copper powder was stabilized with benzoic acids, where the process of Cu powder stabilization was performed in order to protect the powder against subsequent oxidation. It can be concluded that there is no chemical reaction occurring between PLGA and copper powder, and that the influence of the O-H, C=O and C=C groups on the spectra is amplified. The shift in wavenumbers values between the studied samples is minimal.

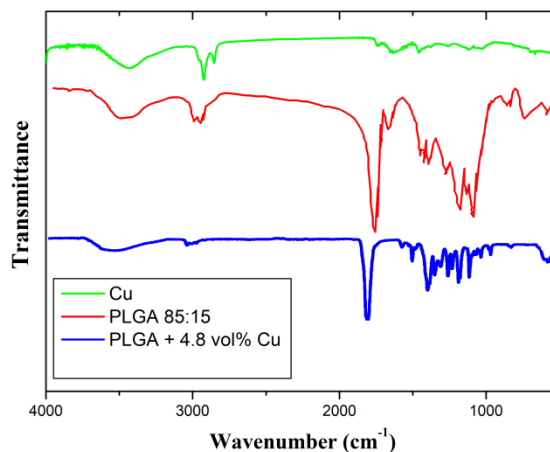


Figure 6. FTIR spectra of the pure stabilized copper powder, PLGA and its composite at 4.8 vol. % Cu content.

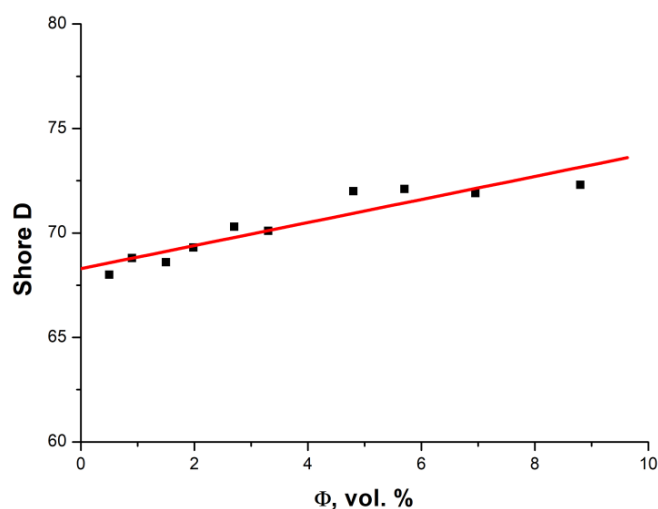


Figure 7. Hardness of copper filled PLGA composites. Measurements are shown as Shore D values

Figure 7 shows the dependence of hardness of different PLGA/Cu composite samples measured as Shore D values. Five data points were taken for each sample and no difference was found between values obtained for both faces of each sample. The hardness of the investigated composites, as

expected, increased with increase in the volume fraction of the copper powder, which has much greater hardness than PLGA polymers.

4. CONCLUSIONS

Experimental study about the effects of morphology and filler volume content of electrodeposited copper powder on the electrical conductivity of PLGA/Cu composites has been described in this article. Results have shown that the powder has well developed high value surface area and that it is dendritic with well-developed primary and secondary dendrite arms. The conductivity measurements showed S-shaped dependency with percolation transition from non-conductive to conductive region, which is typical for these kind of polymer composite systems. The results have shown and confirmed previous researches that the shape and morphology of the filler play a significant role in the phenomenon of electrical conductivity of the prepared samples and the appearance percolation threshold. Conductivity measurements have shown that percolation threshold, measured from maximum of derivative of conductivity, is at 2.72 vol. % Cu. The results showed that conductivity of PLGA composites is much improved comparing to similar composites filled with more regular structure fillers that can be found in the literature. Morphology of the samples showed presence of conductive pathways throughout the sample, which was proven by EDS measurements. Clearly, it was shown that composites conduct electricity throughout conductive pathways that are formed in 3D in pure stochastic order. FTIR measurements have shown that there is no chemical reaction taking place between PLGA and copper powder. The hardness of the investigated composites increased with increase in the volume fraction of the copper powder, since the hardness of the copper is much larger than the hardness of the PLGA polymer.

ACKNOWLEDGEMENT

This work was financially supported by Ministry of Education, Science and Technological Development of the Republic of Serbia under the research projects: ON172046 and ON172060.

References

1. K. Zhang, J. L. Schnoor, E. Y. Zeng, *Environ. Sci. Technol.* 46 (2012) 10861.
2. M. Heacock, C. B. Kelly, K. A. Asante, L. S. Birnbaum, Å. L. Bergman, M.-N. Bruné, I. Buka, D. O. Carpenter, A. Chen, X. Huo, M. Kamel, P. J. Landrigan, F. Magalini, F. Diaz-Barriga, M. Neira, et al., *Environ. Health Perspect.* 124 (2016) 550.
3. B. H. Robinson, *Sci. Total Environ.* 408 (2009) 183.
4. R. Widmer, H. Oswald-Krapf, D. Sinha-Khetriwal, M. Schnellmann, H. Böni, *Environ. Impact Assess. Rev.* 25 (2005) 436.
5. X. Yu, W. Shou, B. K. Mahajan, X. Huang, H. Pan, *Adv. Mater.* 30 (2018) 1707624.
6. K. K. Fu, Z. Wang, J. Dai, M. Carter, L. Hu, *Chem. Mater.* 28 (2016) 3527.
7. H. Cheng, *J. Mater. Res.* 31 (2016) 2549.
8. S. Bauer, M. Kaltenbrunner, *ACS Nano* 8 (2014) 5380.
9. X. Huang, *J. Semicond.* 39 (2018) 11003.

10. S.-W. Hwang, H. Tao, D.-H. Kim, H. Cheng, J.-K. Song, E. Rill, M. A. Brenckle, B. Panilaitis, S. M. Won, Y.-S. Kim, Y. M. Song, K. J. Yu, A. Ameen, R. Li, Y. Su, et al., *Science* (80-.). 337 (2012) 1640.
11. S.-W. Hwang, D.-H. Kim, H. Tao, T. Kim, S. Kim, K. J. Yu, B. Panilaitis, J.-W. Jeong, J.-K. Song, F. G. Omenetto, J. A. Rogers, *Adv. Funct. Mater.* 23 (2013) 4087.
12. Y. Gao, Y. Zhang, X. Wang, K. Sim, J. Liu, J. Chen, X. Feng, H. Xu, C. Yu, *Sci. Adv.* 3 (2017).
13. H. L. Hernandez, S.-K. Kang, O. P. Lee, S.-W. Hwang, J. A. Kaitz, B. Inci, C. W. Park, S. Chung, N. R. Sottos, J. S. Moore, J. A. Rogers, S. R. White, *Adv. Mater.* 26 (2014) 7637.
14. C. H. Lee, S.-K. Kang, G. A. Salvatore, Y. Ma, B. H. Kim, Y. Jiang, J. S. Kim, L. Yan, D. S. Wie, A. Banks, S. J. Oh, X. Feng, Y. Huang, G. Troester, J. A. Rogers, *Adv. Funct. Mater.* 25 (2015) 5100.
15. Y. Gao, K. Sim, X. Yan, J. Jiang, J. Xie, C. Yu, *Sci. Rep.* 7 (2017) 947.
16. C. W. Park, S.-K. Kang, H. L. Hernandez, J. A. Kaitz, D. S. Wie, J. Shin, O. P. Lee, N. R. Sottos, J. S. Moore, J. A. Rogers, S. R. White, *Adv. Mater.* 27 (2015) 3783.
17. X. Zhang, L. M. Bellan, *ACS Appl. Mater. Interfaces* 9 (2017) 21991.
18. S. Çınar, R. Jamshidi, Y. Chen, N. Hashemi, R. Montazami, *J. Polym. Sci. Part B Polym. Phys.* 54 (2016) 517.
19. S.-W. Hwang, G. Park, H. Cheng, J.-K. Song, S.-K. Kang, L. Yin, J.-H. Kim, F. G. Omenetto, Y. Huang, K.-M. Lee, J. A. Rogers, *Adv. Mater.* 26 (2014) 1992.
20. C. M. Boutry, A. Nguyen, Q. O. Lawal, A. Chortos, S. Rondeau-Gagné, Z. Bao, *Adv. Mater.* 27 (2015) 6954.
21. K. J. Yu, D. Kuzum, S.-W. Hwang, B. H. Kim, H. Juul, N. H. Kim, S. M. Won, K. Chiang, M. Trumpis, A. G. Richardson, H. Cheng, H. Fang, M. Thompson, H. Bink, D. Talos, et al., *Nat. Mater.* 15 (2016) 782.
22. S.-K. Kang, R. K. J. Murphy, S.-W. Hwang, S. M. Lee, D. V Harburg, N. A. Krueger, J. Shin, P. Gamble, H. Cheng, S. Yu, Z. Liu, J. G. McCall, M. Stephen, H. Ying, J. Kim, et al., *Nature* 530 (2016) 71.
23. D. Son, J. Lee, D. J. Lee, R. Ghaffari, S. Yun, S. J. Kim, J. E. Lee, H. R. Cho, S. Yoon, S. Yang, S. Lee, S. Qiao, D. Ling, S. Shin, J.-K. Song, et al., *ACS Nano* 9 (2015) 5937.
24. H. Tao, S.-W. Hwang, B. Marelli, B. An, J. E. Moreau, M. Yang, M. A. Brenckle, S. Kim, D. L. Kaplan, J. A. Rogers, F. G. Omenetto, *Proc. Natl. Acad. Sci.* 111 (2014) 17385.
25. R. P. Félix Lanao, A. M. Jonker, J. G. C. Wolke, J. A. Jansen, J. C. M. van Hest, S. C. G. Leeuwenburgh, *Tissue Eng. Part B. Rev.* 19 (2013) 380.
26. L. Yu, J. Ding, *Chem. Soc. Rev.* 37 (2008) 1473.
27. H. Shen, X. Hu, J. Bei, S. Wang, *Biomaterials* 29 (2008) 2388.
28. E. Swider, O. Koshkina, J. Tel, L. J. Cruz, I. J. M. de Vries, M. Srinivas, *Acta Biomater.* 73 (2018) 38.
29. J. Yang, G. Shi, J. Bei, S. Wang, Y. Cao, Q. Shang, G. Yang, W. Wang, *J. Biomed. Mater. Res.* 62 (2002) 438.
30. H. Zhang, J. Wang, K. Wang, L. Xu, *Mater. Lett.* 212 (2018) 118.
31. V. H. Poblete, M. P. Alvarez, V. M. Fuenzalida, *Polym. Compos.* 30 (2009) 328.
32. Y. P. Mamunya, V. V Davydenko, P. Pissis, E. V Lebedev, *Eur. Polym. J.* 38 (2002) 1887.
33. E. P. Mamunya, V. V Davydenko, E. V Lebedev, *Compos. Interfaces* 4 (1996) 169.
34. Z. Janković, M. M. Pavlović, M. R. P. Pavlović, M. G. Pavlović, N. D. Nikolić, J. S. Stevanović, S. Pršić, *Int. J. Electrochem. Sci.* 13 (2018) 291.
35. M. M. Pavlović, M. G. Pavlović, V. Cosović, V. Bojanić, N. D. Nikolić, R. Aleksić, *Int. J. Electrochem. Sci.* 9 (2014) 8355.
36. M. M. Pavlovic, V. Cosovic, M. G. Pavlovic, V. Bojanic, N. D. Nikolic, R. Aleksic, *Int. J. Electrochem. Sci.* 7 (2012) 8883.
37. Z. Janković, M. M. Pavlović, M. R. Pantović Pavlović, N. D. Nikolic, V. Zečević, M. G.

- Pavlović, *Hem. Ind.* 72 (2018) 285.
38. M. M. Pavlović, V. Čosović, M. G. Pavlović, N. Talijan, V. Bojanić, *Int. J. Electrochem. Sci.* 6 (2011).
 39. Y. Nishi, Y. Ebihara, N. Kunikyoh, M. Kanda, K. Iwata, K. Yuse, B. Guiffard, L. Lebrun, D. Guyomar, *Mater. Trans.* 51 (2010) 1437.
 40. A. F. Osman, M. Mariatti, *Polym. Polym. Compos.* 14 (2006) 623.
 41. A. S. Luyt, J. A. Molefi, H. Krump, *Polym. Degrad. Stab.* 91 (2006) 1629.
 42. G. Pinto, A.-K. Maaroufi, R. Benavente, J. M. Perena, *Polym. Compos.* 32 (2011) 193.
 43. Y. Baziard, S. Breton, S. Toutain, A. Gourdenne, *Eur. Polym. J.* 24 (1988) 521.

© 2019 The Authors. Published by ESG (www.electrochemsci.org). This article is an open access article distributed under the terms and conditions of the Creative Commons Attribution license (<http://creativecommons.org/licenses/by/4.0/>).